

Conclusions

These results demonstrate that the use of larger second pulse fractions in the presence of a large bias in the track (that is, greater than the KKV divert) can reduce the requirements on the weapon system by allowing the bias in the target track to be removed later during the flight. Additionally, the 50/50-pulse split extends both the minimum and maximum feasible mission times relative to the 80/20-pulse split. This increases the engagement envelope of the interceptor in the presence of a large bias in the target track.

Reference

¹Phillips, C. A., and Malyevac, D. S., "Pulse Motor Optimization via Mission Charts for an Exoatmospheric Interceptor," *Journal of Guidance, Control, and Dynamics*, Vol. 21, No. 4, 1998, pp. 611-617.

Nonlinear Entry Trajectory Control Using Drag-to-Altitude Transformation

Shinji Ishimoto*

National Aerospace Laboratory,
Chofu, Tokyo 182-8522, Japan

I. Introduction

EXISTING entry guidance systems are based on the common concept of tracking a reference drag profile. For that purpose, trajectory control laws are incorporated into the guidance systems. A linear control law has been employed successfully for the Space Shuttles.¹ This control law was designed with a classical method based on linearized equations of motion. This approach generally needs gain schedules interpolating feedback gains selected at individual design points. However, it is not an easy task to prepare such gain-scheduling functions that give a satisfactory performance over the whole entry phase. Motivated by this fact, many authors recently have proposed nonlinear trajectory control laws.²⁻⁵ These control laws were developed with the feedback linearization (or dynamic inversion) method⁶ or related methods. Design parameters of these techniques are some constants describing a desired response independent of reference values. Therefore, extensive gain schedules are not necessary. For this reason, nonlinear control laws will be the mainstream for entry guidance in place of linear control laws. A new nonlinear control law is proposed using a device called the altitude-to-drag transformation. The altitude instead of the drag force is considered as the controlled variable. The new nonlinear control law is described and numerically compared with a conventional linear control law.

II. Nonlinear Trajectory Control Law

A. Basic Control Law

The primary function of entry trajectory control laws is to modulate the bank angle (roll angle around the atmospheric-relative velocity). The control law proposed in the note is summarized as

$$\ddot{h}_C = \ddot{h}_{\text{REF}} + f_1 h_{\text{ERR}} + f_2 \dot{h}_{\text{ERR}} + f_3 \int h_{\text{ERR}} dt \quad (1)$$

$$(L/D)_C = \ddot{h}_C / D + \dot{h} / V + (g/D)(1 - V^2 / V_S^2) \quad (2)$$

$$\phi_C = \cos^{-1} \left[\frac{(L/D)_C}{L/D} \right] \quad (3)$$

Received 14 June 1999; presented as Paper 99-4169 at the AIAA Atmospheric Flight Mechanics Conference, 9-11 August 1999; revision received 26 September 1999; accepted for publication 30 September 1999. Copyright © 1999 by the American Institute of Aeronautics and Astronautics, Inc. All rights reserved.

*Senior Researcher, Flight Research Division, 7-44-1 Jindaijihigashimachi. Member AIAA.

where D is the drag force per unit mass (also termed drag acceleration), g is the acceleration due to gravity, h is the altitude, \dot{h} is the altitude rate, \ddot{h} is the vertical acceleration, L/D is the lift-to-drag ratio, V is the Earth-relative velocity, V_S is the circular orbital velocity, and ϕ is the bank angle. The subscripts C , ERR , and REF stand for a command, an error, and a reference value, respectively. The symbols without any subscripts denote real-time measurements. The feedback gains, f_1 , f_2 , and f_3 , characterize the desired vertical acceleration \ddot{h}_C for attenuating the altitude error h_{ERR} . The intermediate lift-to-drag ratio command $(L/D)_C$ is a normalized version of the vertical component of lift force required for trajectory control. The mapping function (2) is based on the following equation of motion in the vertical direction

$$\ddot{h} = -D(h/V) + L \cos \phi - (g/D)[1 - (V^2 / V_S^2)] \quad (4)$$

where L is the lift force per unit mass. Correspondence between Eqs. (2) and (4) is obvious, since $L \cos \phi$ in Eq. (4) represents the vertical component of lift force.

B. Tracking Error

The errors used in the control law (1) are defined as

$$h_{\text{ERR}} = h_{\text{REF}} - h_D \quad (5)$$

$$\dot{h}_{\text{ERR}} = \dot{h}_{\text{REF}} - \dot{h} \quad (6)$$

where h_D is a pseudo-altitude derived from the drag acceleration, and \dot{h} is an altitude rate estimated by a navigation system. The reference altitude h_{REF} and the drag-derived altitude h_D are computed from the common models for the drag force and atmospheric density

$$D = [\rho V^2 S C_D(V)] / 2m \quad (7)$$

$$\rho = \rho_0 \exp(-h/h_S) \quad (8)$$

where C_D is the drag coefficient, h_S is the atmospheric density scale height, m is the vehicle mass, S is the vehicle reference area, ρ is the atmospheric density, and ρ_0 is the atmospheric density at sea level. In general, C_D is a function of the angle of attack α and the Mach number. However, the atmospheric-relative velocity is almost equal to V , and the speed of sound is nearly constant during entry. In addition, we assume that α is scheduled as a function of V . Therefore, C_D is described as a function of only V as shown in Eq. (7).

When the reference drag D_{REF} is a function of the specific energy (energy per unit mass) E , the altitude error h_{ERR} is explicitly written as

$$h_{\text{ERR}} = -h_S [\log(D_{\text{REF}}/D)] W_2 \quad (9)$$

$$W_1 = 1 + (V/2)(C'_D / C_D) \quad (10)$$

$$W_2 = [1 + (2gh_S / V^2) W_1]^{-1} \quad (11)$$

where C'_D represents $\partial C_D / \partial V$. If D_{REF} is a function of V , we do not need W_2 in Eq. (9). The scale height h_S is generally scheduled as a function of the altitude based on a standard atmosphere. Equation (9) can be derived from Eqs. (7) and (8) by using the relation:

$$E = \frac{1}{2} V^2 + gh = \frac{1}{2} V_{\text{REF}}^2 + gh_{\text{REF}} \quad (12)$$

and the assumption $gh_{\text{ERR}} \ll V^2$, which usually holds during entry.⁷

Linearizing Eq. (9) about D_{REF} , we obtain the following expression:

$$h_{\text{ERR}} \cong -h_S (W_2 / D_{\text{REF}}) (D_{\text{REF}} - D) \quad (13)$$

If this formula is adopted for mapping the drag error into h_{ERR} , the control law as shown in Eq. (1) becomes equivalent to a conventional linear control law.¹ Equation (13) implies that the scale height h_S works as a part of the feedback gain with respect to the drag error. The inaccuracy of h_S included in the reference altitude rate \dot{h}_{REF} (the definition is shown later) causes a steady-state tracking error, but this error is eliminated by the integral term in Eq. (1). Therefore,

the deference between a scheduled profile of h_S and an actual profile encountered during entry does not significantly degrade the performance in terms of tracking drag profiles.

C. Reference Trajectory Parameters

If the reference drag D_{REF} is a function of the energy E , the reference trajectory parameters are defined as follows:

$$\dot{D}_{\text{REF}} = \frac{\partial D_{\text{REF}}}{\partial E} (-V D_{\text{REF}}) \quad (14)$$

$$\dot{V}_{\text{REF}} = \left(-D_{\text{REF}} + \frac{g h_S \dot{D}_{\text{REF}}}{D_{\text{REF}} V} \right) W_2 \quad (15)$$

$$\dot{h}_{\text{REF}} = -h_S \left(\frac{\dot{D}_{\text{REF}}}{D_{\text{REF}}} + \frac{2 D_{\text{REF}}}{V} W_1 \right) W_2 \quad (16)$$

$$\ddot{D}_{\text{REF}} = \frac{\partial^2 D_{\text{REF}}}{\partial E^2} (-V D_{\text{REF}})^2 + \frac{\partial D_{\text{REF}}}{\partial E} (-\dot{V}_{\text{REF}} D_{\text{REF}} - V \dot{D}_{\text{REF}}) \quad (17)$$

$$\begin{aligned} \ddot{h}_{\text{REF}} = h_S & \left[-\frac{\dot{D}_{\text{REF}}}{D_{\text{REF}}} + \frac{\dot{D}_{\text{REF}}^2}{D_{\text{REF}}^2} + \frac{2}{V} \left(\frac{g h_{\text{REF}} \dot{V}_{\text{REF}}}{V^2} - \dot{D}_{\text{REF}} \right) W_1 \right. \\ & \left. + \frac{2}{V^2} \left(\frac{g h_{\text{REF}} \dot{V}_{\text{REF}}}{V} + \dot{V}_{\text{REF}} D_{\text{REF}} \right) \left(1 + \frac{V^2}{2} \frac{C_D^2}{C_D^2} \right) \right] \end{aligned} \quad (18)$$

In these equations, we use the measured velocity V in place of the reference velocity V_{REF} , because the difference between these parameters is generally small. We immediately obtain Eq. (18) by differentiating Eq. (16) based on the assumption $C_D'' = 0$. Equations (15) and (16) are derived from the following differential equations⁷:

$$\dot{h} = h_S [-\dot{D}/D + 2\dot{V}/V + (C_D'/C_D)\dot{V}] \quad (19)$$

$$\dot{V} = -D - g \sin \gamma = -D - g(h/V) \quad (20)$$

where γ is the flight path angle. Equation (20) is the equation of motion with respect to V , and Eq. (19) is obtained by differentiating Eq. (7) with respect to time. In addition, the following differential equation is applied to Eq. (14).⁷

$$\dot{E} = -V D \quad (21)$$

D. Discussion on Controlled Variable

A drawback in tracking reference drag profiles is that the altitudes at the end of entry guidance widely disperse because of the variations of atmospheric density. This interface altitude error is probably reduced (i.e., guidance capability is improved) by the feedback of a geometrical altitude error during a final portion of the entry guidance phase. The control law in Eq. (1) is able easily to deal with the geometrical altitude error as well as the fictitious altitude error converted from the drag error. This is a potential advantage for selecting the altitude instead of the drag force as the controlled variable. A trajectory control law employing a blend of the true and drag-derived altitude errors is under investigation.

III. Numerical Comparison

We conducted three-degree-of-freedom (3DOF) flight simulations numerically to compare the new nonlinear control law with a conventional linear control law.

A. Simulation Models

We employed the Hypersonic Flight Experiment (HYFLEX) vehicle as a vehicle model for numerical simulation. The hypersonic research aircraft was developed by the National Aerospace Laboratory (NAL), Japan and the National Space Development Agency of Japan (NASDA). The three-view drawing is shown in Fig. 1. The HYFLEX vehicle was launched by a small booster, and successfully performed a hypersonic gliding flight in 1996. For the flight test, we

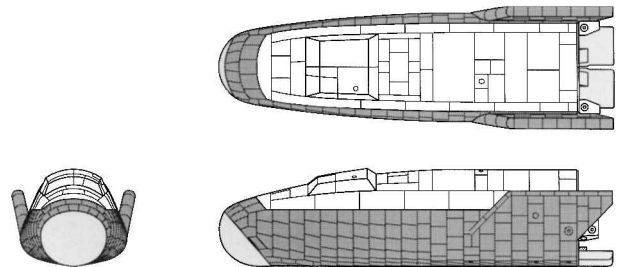


Fig. 1 NAL/NASDA HYFLEX vehicle.

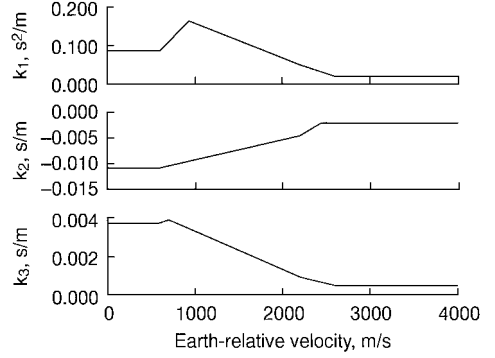


Fig. 2 Scheduled gains for linear control law.

developed the following linear trajectory control law similar to that of the Space Shuttle⁸:

$$\begin{aligned} \left(\frac{L}{D} \right)_C &= \left(\frac{L}{D} \right)_{\text{REF}} + k_1(D - D_{\text{REF}}) + k_2(h - h_{\text{REF}}) \\ &+ k_3 \int (D - D_{\text{REF}}) dt \end{aligned} \quad (22)$$

Figure 2 presents the scheduled gains k_1 , k_2 , and k_3 for this equation. We chose the flight-proven control law in Eq. (22) as one of the compared control laws. The other is the nonlinear control law described in the previous section. For a neutral comparison, the feedback gains of the nonlinear control law were determined so as to give a comparable response to the linear control law. The feedback gains in Eq. (1) were taken as $f_1 = 0.004$, $f_2 = 1.6\sqrt{f_1}$, and $f_3 = f_1/50$ (gain-scheduling functions were not needed). For both control laws, we used the following reference drag profile that had been developed for the HYFLEX vehicle:

$$D_{\text{REF}} = D_F + C_1(E - E_F) \quad (23)$$

where C_1 , D_F , and E_F are constants. In each simulation, a trajectory was computed over a period from an Earth-relative velocity of 2200 m/s (about Mach 7) to a Mach number of 3.0. In addition, the actual attitudes were assumed to be equal to the commands.

B. Simulation Results

Figure 3 shows a comparison of the drag profiles under the linear and nonlinear control laws. The horizontal axes in this figure represent the energy per unit mass, and the reference drag profiles are plotted as straight broken lines. The actual drag profiles were computed for different initial altitudes (Δh in Fig. 3 indicates a perturbation from a nominal initial condition). All of the responses are regarded as acceptable, though somewhat large overshoots are observed. Remarkable differences are not found between the linear and nonlinear control laws. However, the responses under the linear control law slightly deviate below the reference drag profile. Nonlinearity disregarded by linearization process or some errors included in the reference parameters may cause this phenomenon. Both control laws were tested against various uncertainties, but significant differences were not observed. This simulation study shows that the new nonlinear control law has satisfactory performance and robustness, and it can be used as a superior substitute of conventional linear control laws.

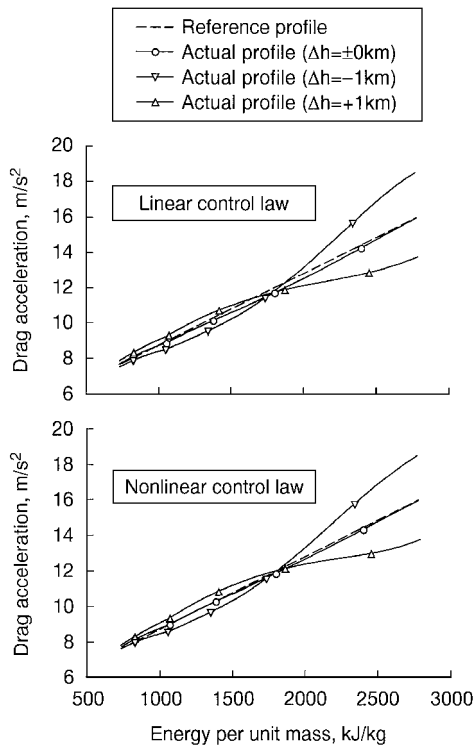


Fig. 3 Comparison of drag profiles under linear and nonlinear control laws (Δh : initial perturbation of altitude from nominal condition).

IV. Conclusions

This Note presented a new nonlinear trajectory control law to track a reference drag profile used for entry guidance. We introduced a device called the drag-to-altitude transformation and showed that a trajectory control law can be formulated based on the equation of motion with respect to altitude. A potential advantage of this approach is the capability of handling the geometrical altitude along with the drag-derived altitude. We are developing an advanced control law to make use of this point. The feedback of geometrical altitude would be effective for reducing altitude errors at the end of entry guidance.

References

- ¹Harpold, J. C., and Graves, Jr., C. A., "Shuttle Entry Guidance," *The Journal of the Astronautical Sciences*, Vol. 27, No. 3, 1979, pp. 239-268.
- ²Mease, K. D., and Kremer, J.-P., "Shuttle Entry Guidance Revisited Using Nonlinear Geometric Methods," *Journal of Guidance, Control, and Dynamics*, Vol. 17, No. 6, 1994, pp. 1350-1356.
- ³Roenneke, A. J., and Well, K. W., "Nonlinear Drag-Tracking Control Applied to Optimal Low-Lift Reentry Guidance," AIAA Paper 96-3698, July 1996.
- ⁴Hanson, J. M., Coughlin, D. J., Dukeman, G. A., Malqueen, J. A., and McCarter, J. W., "Ascent, Transition, Entry, and Abort Guidance Algorithm Design for the X-33 Vehicle," AIAA Paper 98-4409, Aug. 1998.
- ⁵Lu, P., and Hanson, J. M., "Entry Guidance for the X-33 Vehicle," *Journal of Spacecraft and Rockets*, Vol. 35, No. 3, 1998, pp. 342-349.
- ⁶Slotine, J.-J. E., and Li, W., *Applied Nonlinear Control*, Prentice-Hall, Upper Saddle River, NJ, 1991, pp. 207-275.
- ⁷Ishimoto, S., "Nonlinear Trajectory Control Using Drag-to-Altitude Transformation for Entry Guidance," AIAA Paper 99-4169, Aug. 1999.
- ⁸Ishimoto, S., Takizawa, M., Suzuki, H., and Morito, T., "Flight Control System of Hypersonic Flight Experiment Vehicle," AIAA Paper 96-3404, July 1996.